Structural Topology Optimisation with R-Snakes Volume of Solid

A. D. J. Taylor * A. D. J. Payot † ; C. B. Allen ‡ ; T. C. S. Rendall §
Department of Aerospace Engineering, University of Bristol, Bristol, UK

A topologically flexible parameterisation method developed for aerodynamic optimisation is tested on a variety of 2 dimensional structural topology problems. The background to the restricted snakes volume of solid (RSVS) is explained. A topology optimisation framework is develloped using FreeFem++ as a linear elastic solver and differential evolution as the agent based optimiser. Validation of the analysis is presented as well as mesh convergence and impact studies. The work here is significant such that if a parameterisation method is capable of both aerodynamic and structural optimisation, the potential for multidisciplinary analysis arises. Structural topology optimisation of volume constrained agent-based optimisation, minimising deflection, has been run on four common benchmark cases; two short cantilever beams and two longer centrally loaded (MBB) beams. Results were compared to SIMP calculations made following using Sigmund's 99 line topology optimisation code [1]. RSVS solutions scored objective functions comparable to those found via SIMP in all cases with differences ranging from +40% to -5%. In the long run the combined capability of the RSVS in aerodynamics and structures offers the potential of the development of a general aero-structural topology optimisation framework using a single set of design variables.

I. Introduction

Prediction of structural and aerodynamic behaviour using numerical modes is now commonplace in industry and academia. Correctly exploiting the capabilities of finite element analysis (FEA) and computation fluid dynamic (CFD) tools is an integral part of the modern engineers skill-set. Exploiting these methods automatically, numerical optimisation has emerged as a powerful way of exploring and understanding physical design spaces. In structural design, this is most obvious through the extreme topological complexity and geometrical flexibility allowed by modern topology optimisation methods [2]. Progress in aerodynamic shape optimisation has focused on increasingly refining the conventional aircraft configuration [3, 4]. Significant steps towards improved designs through the use of standard test cases of AIAA Aerodynamic Design Optimisation Discussion Group (ADODG) [5].

A successful design optimisation framework relies on parameterisation of the design space, accurate physics calculation, and a robust optimiser. During parameterisation the design variables, forming a numerical vector understood by the optimiser, are converted into a geometry exploitable by the physical model. Requirements on parameterisation methods vary with enormously with application leading to extreme differences in capability. In external aerodynamics, *shape* parameterisation methods only represent one type of shape, with a great degree of accuracy. *Topology* parameterisation methods, common in structural applications, have control over a much more varied design space: the parameterisation supports changes in the number of bodies and holes within a design.

In structural optimisation the exploration of topology is commonplace with SIMP, ESO and level set methods (LSMs) all well established in academia and industry. Restricted snakes volume of solid (RSVS) is a parameterisation method, recently developed by the authors, which brings topological flexibility to traditional aerodynamic optimisation frameworks [6, 7]. In this work the authors use the RSVS to tackle 2-dimensional structural topology optimisation problems.

This parameterisation is at the intersection of level sets and density methods: it interprets coarse volume of solid information into a crisp, smooth boundaries. It requires relatively small numbers of design variables and provides good control and flexibility in the distribution of those design variables through geometric space. Geometries constructed using RSVS can also be shown to have equivalent non-uniform rational b-spline (NURBS) definitions, making the method compatible with some existing CAD definitions. Compactness is of paramount importance in aerodynamic parameterisation; this has led to a number of hierarchical approaches to design variables with excellent results on the

*Undergraduate Student, at14135@my.bristol.ac.uk, Bristol, BS8 1TR, UK
†PhD Student, AIAA Student Member, a.payot@bristol.ac.uk, Bristol, BS8 1TR, UK
‡Professor of Computational Aerodynamics, AIAA Senior Member, c.b.allen@bristol.ac.uk, Bristol, BS8 1TR, UK
§Lecturer, AIAA Member, thomas.rendall@bristol.ac.uk, Bristol, BS8 1TR, UK

convergence speed of high-resolution optimisation problems [8–11]. This is similar to the approaches of Maute and Ramm [12], Kim et al. [13] and Bandara et al. [14] in STO. This method was developed with a hierarchical approach to design variables [7], allowing a progressive increase in geometric fidelity as the optimisation progresses and permitting design flexibility beyond that originally specified by the designer, and, reducing the amount of set-up for a user of the RSVS optimisation framework.

The authors' previous publications outline this method and demonstrate its performance in aerodynamic optimisation [6, 7, 15]. The RSVS has recently been extended to 3 dimensions. In this work, the method is successfully trialled for structural topology optimisation. The results of this will point towards whether this method could be used in an aero-structural optimiser, where the structural and aerodynamic features share one common set of design variables. This could be applied in situations where aero-structural interactions dominate, for example: winglets, internal engine components or hydrofoils. This document is organised as follows: section II presents the relevant background; section III presents the a summary of the key features of the Restricted Snakes Volume of Solid method; section IV details the key considerations of the implementation and analysis of an STO framework using RSVS; section V presents the initial structural optimisation results obtained.

II. Background

Structural Topology Optimisation

The first work on structural Topology Optimisation (STO) dates back to 1904 where Michell devised analytically curved optimal shapes [16], which share properties with the shapes found numerically today. It was then through a seminar paper in 1988 when Bendsøe and Kikuchi introduced numerical methods in STO through homogenization methods [17]. Since then, the field has developed significantly, seeing successful industrial applications of structural topology optimisation. In the aerospace domain, through topological optimisation of the fuselage door intercostals, and the inner and outer leading edge ribs, 700-1000kg of weight was saved on the A380 [18]. Boeing have also used structural STO for optimising the underfloor beams of the CH-47 Chinook helicopter [19]. Methods in the field are split into three broad categories: density based methods, discrete methods and level set methods (LSMs).

Homogenization methods include SIMP (Solid Isotropic Material with Penalization) and ESO (Evolutionary Structural Optimisation), both having reached the stage of application in industrial software [20]. These methods discretise the design space into a finite number of elements used directly for structural analysis. SIMP avoids the binary nature of the problem (i.e. solid = 1, void = 0) by introducing a continuous density variable, ρ, for each element, which can conceptually be thought of as increased porosity of the material. A penalty function is then used to penalise the intermediate densities ($0 < \rho < 1$), to obtain an almost entirely binary design space [21]. Disadvantages of this method come from the intermediate densities that remain: non-smooth borders of the resulting topology, and the difficulty of converting the output geometry into a manufacturable model [21]. SIMP was used to optimise a full Boeing 777 wing under aerodynamic loads by Aage et al. [2]. This results showed an unrivalled combination of scale and resolution, leading to some structures reminiscent of internal bone structures of birds.

ESO falls into the category of 'hard kill', discrete methods. At its simplest level, every iteration ESO calculates a criterion function for each element (usually von Mises stress), and then removes elements with the lowest criterion function [22]. One of the criticism of ESO is that the method is fully heuristic, meaning no proof exists that the process described above leads to an optimal solution [20]. Other criticisms refer to the difficulty in applying constraints such as stress or displacement [22], and how volume control can result in a highly non-optimal solution [20].

Level-set-methods (LSM) are the other major class of STO methods [23]. LSM work by implicitly defining the structural borders through contours of a Level-set function (LSF). Unlike homogenization methods, these provide a crisp border for designers to work with [23]. These approaches consist of three main stages: parameterising the LSF, mapping the geometry to the mechanical model, and the updating process for the optimisation. Shape sensitivities are used to alter the shape; a merit function is found from moving the boundaries in the normal direction [23]. Topological derivatives, also known as the bubble method, which first emerged in 1994 [24], are used to guide the introduction of holes in the geometry. These methods predict the effect of adding infinitesimal holes at points, and use this information to produce new holes in the solid [24]. This introduction of holes gives LSMs the required topological flexibility, but affects the convergence of the process [25]. Overall the main disadvantage of LSMs is the dependency of the final results on the initial estimate [25–27].

All of these methods have been used in 2 and 3 dimensions [2, 28, 29]. For more information on the development and use of these methods, the reader is referred to the general review papers by Deaton and Grandhi [30] and Sigmund [25], and, for more detail on level set methods to Van Dijk et al. [23].

Both homogenization methods [31, 32] and level set methods [33, 34] have been adapted to fluid topology optimisation in 2 and 3 dimensions. Modelling the Stokes equations and incompressible flows at low Reynolds numbers,

solved by finite element elasticity solvers, these methods have yielded good results on the optimization of microfluidic devices and channel flows [32, 35]. Unfortunately these methods, with the exception of the cutFEM method by Villanueva et al. [34] do not maintain a smooth and crisp fluid boundary limiting their use for compressible aerodynamics which use solutions to the Euler and compressible Reynolds averaged Navier-Stokes (RANS) equations at high Reynolds numbers.

Aerodynamic Shape Optimisation

The three main components of ASO are parameterisation, CFD (objective function analysis), and the optimiser. These include other important aspects such as mesh generation and deformation, and constraint handling; which come with their own suite of challenges. As these disciplines remain active research fields in their own right a modular approach to ASO is the norm, allowing future developments to be easily integrated with current methods. This is different to most STO frameworks which are fully integrated, with parameterisation, meshing and solving often performed on the same discretisation.

Parameterisation methods need to contain flexibility with regard to the geometries they can produce, whilst possessing as few design variables (parameters) as possible. Specifically, aerodynamic parameterisation methods need to represent common aerodynamic features, such as smoothness of the surfaces, and sharp corners at the trailing or leading edges. Fewer parameters mean computationally cheaper frameworks, as fewer parameters mean optimisers converge more rapidly.

Parameterisation methods can generally be split into two categories, constructive and deformative. Constructive methods are able to represent geometries from only the design variables, these include CST [36] and PARSEC [37]. Deformative methods specify changes away from a known geometry, a non-exhaustive list includes: Hicks-Henne bump functions [38], Free Form Deformation (FFD) methods [39], data base singular value decomposition (SVD) [40] and subdivision curves [41]. Constrained smooth mesh-point movement can also be used to control the evolution of the geometry [42]. Many of these parameterisation are directly compared inside a single ASO framework, in geometric and aerodynamic terms, in [43] and [44] respectively. Conventional parameterisation methods in ASO are only capable of shape parameterisation. The cost of CFD evaluation and the need to keep the number objective function calls has led to the emergence of approaches to reduce the number of design variables. Methods such as surrogate based optimisation, active sub-space methods and hierarchical design variables have yielded good results with reduced computational cost. The RSVS parameterisation used in this work is based of previous work in volume of solid (VOS) based parameterisation by Hall et al. [45]. This work was extended into a parameterisation with accurate and consistent shape response to small changes of design variables as well as topological flexibility.

In ASO gradient based optimisation is most common, it offers fast and reliable convergence. SNOPT [46] is a widely used Sequential Quadratic Programming (SQP) code used in the ASO community [4, 15, 44, 47–49]. The adjoint method, developed by Pironneau [50] and popularised in ASO by Jameson [51], was a major breakthrough in the field of optimisation. This ensures the computation time for each gradient calculation is independent of the number of design variables. Convergence of SQP based algorithms may be further accelerated by using approximate Hessians when using small numbers of design variables [49]. These offer faster convergence than agent-based methods, but cannot guarantee the global minima will be found, meaning that the final answer depends on the initial estimate. Agent-based optimisation can search the whole design space at greater computational expense, but can make efficient use of parallel computing [52]. Their use is restricted in ASO by computational expense. This consideration has limited their use to explorations of the modality of the aerodynamic design space [15, 48, 53–56]. These studies provide mounting evidence that ASO design spaces are at least somewhat multi-modal.

ASO has shown its capability to explore problems of industrial interest: Allen et al. [57] optimised a helicopter blade in hover, yielding a blade tip shape resembling closely that of the British Experimental Rotor Program (BERP) used on the Leonardo Lynx [57]. Gagnon et Zing, started with a half-sphere and produced a Blended-Wing-Body (BWB) shape, through optimising lift over drag [58], showing the exploratory capabilities of current methods. Bourdette and Martins [4] have been able to show the potential weight benefits through load alleviation of morphing trailing edges on a full aircraft configuration.

Multidisciplinary Optimisation

Aircraft design brings together a large number of disciplines. Conventional optimisation may find optimal solutions to single discipline problems but these may be unusable in practical cases. This is particularly the case for topologically optimal results for aerodynamics which may require some structurally infeasible concepts. *Concurrent* multidisciplinary optimisation allows the optimisation of two or more *coupled* disciplines: the interactions of these disciplines is explored by the optimiser. The difficulty of this task occurs through the need to couple the design variables of the

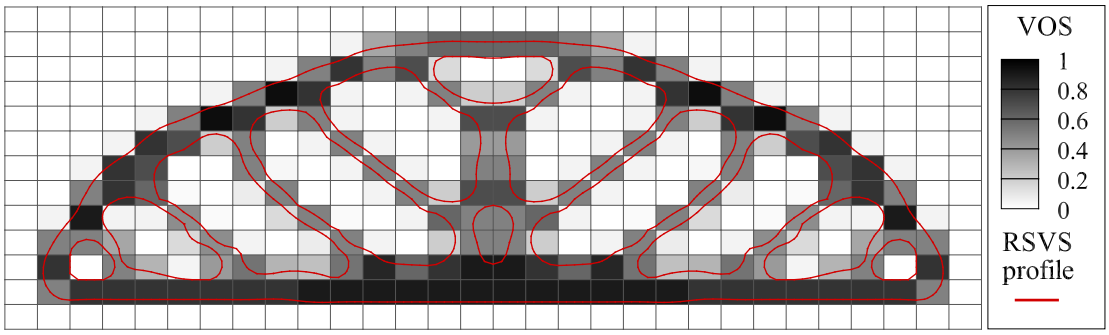

Figure 1. Volume of solid (VOS) design variables as grey-scale and RSVS profile in red; 1 corresponds to a completely full cell and 0 an empty cell, volume fraction distribution was manually designed.

two disciplines together, for the optimiser to control. Various methods exist to control aerodynamic and structural behaviour in one optimisation process. For example, Martins et al. [59] split the design variables into two sets, one set controls the aerodynamic surface, and another controls the thickness of a predetermined structural layout. Kieboom et al. [60] use a similar method, but split the design variables into five groups, of which one controls the structural layout of the wingbox, by changing the panel thickness. Methods such as these tend to use hundreds of design variables and use local optimisation. These are limited in their flexibility and their application to different optimisation problems. A long term goal of the authors for the RSVS parameterisation method is to allow multidisciplinary aero-structural optimisation using a single parameterisation. More information on multidisciplinary optimisation can be found in the review paper by Martins [61].

Motivation & Objectives

The objective of this work is to explore the RSVS method for optimisation of structural profiles. Using common benchmark problems in the structural optimisation field, an STO framework is developed using an open finite element solver, FreeFem++. These results are compared against a SIMP method and show convergence on topologies of similar performance for the RSVS and the SIMP approach. Beyond the multi-disciplinary aspirations of the RSVS methods, it is conceptually interesting in STO as it provides a means of translating VOS/density information to a well defined profile. A potential application of the RSVS would be for the interpretation of density based methods into manufacturable models in 2 and 3 dimensions.

III. Restricted Snakes Volume of Solid

The role of the parameterisation method is to provide an efficient interface between the optimisation method and a fluid or structural solver. This section develops the R-snake volume of solid (RSVS) parameterisation method, which blends the topological flexibility of volume of solid design variables with the requirements of aerodynamic parameterisation methods, primarily the capability to generate smooth surfaces fulfilling volumes specified on a predefined grid. To ensure the method is flexible enough to support anisotropic design variable refinement and to facilitate the extension to 3-dimensions, RSVS must be generic enough to work on arbitrary polygonal grids.

To define a set of VOS variables a grid is superimposed on the design space, where the design variables become the fraction of each cell within a geometry built from this information. This process is shown for a simple grid in figure 1. This parameterisation procedure provides intuitive handling of topology change without explicit control of it, allowing topological flexibility while maintaining smooth control close to topology changes.

$$\begin{aligned} \min \quad & \oint \sqrt{1 + y'^2}\, dx \\ \text{s.t.} \quad & \oint \left(y \cap B_j \right) dx = A_j \qquad \forall j \in \{0, \cdots, m\} \end{aligned} \tag{1}$$

The R-Snake Volume of Solid (RSVS) parametrisation method relies on a restricted snake (r-snake), a type of parametric active contour, to represent geometric profiles. The r-snake is a closed contour composed of connected vertices called snaxels, constrained to travel over the edges of a predefined grid. The movement of these snaxels is governed by a number of simple rules that allow a large range of shapes to be represented and evolved efficiently.

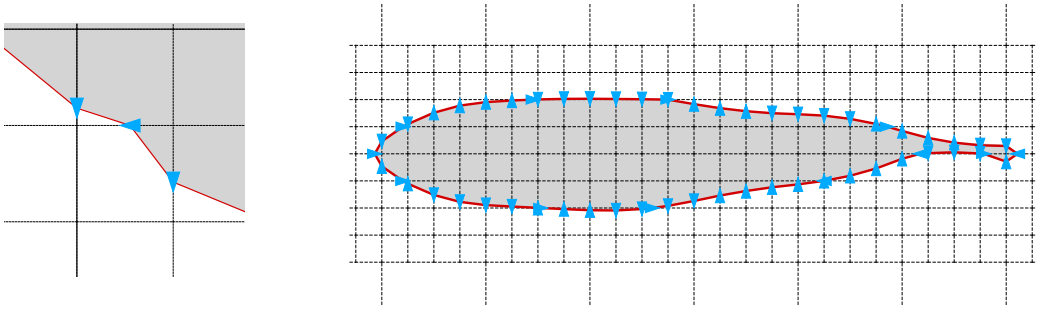

a) Close-up view of snake and snaxel

b) Full view of a closed r-snake

Figure 2. R-snake contour (in red) with snaxels (in blue) evolving on the snaking grid (dashed line).

The current work uses the parametric active contour developed by Bischoff and Kobbelt in [62] for restricted snakes (r-snakes) and an example r-snake with snaxels and the snaking grid is shown in figure 2.

The RSVS governing equation (eq. 1) minimises the length of the profile, while it is also constrained exactly fulfil volumes specified by the VoS design variables. This formulation allows analytical properties of the profiles to be determined using the calculus of variations. It can be shown that this minimisation problem leads to the profile consisting of patched arcs of circles, which can themselves be represented by a continuous NURBS. The r-snake was chosen as it provides efficient topology handling and is tolerant of any convex layout of VOS design variables. Although independent parts of the problem, the governing equation and the contour recovery method can be integrated very efficiently using sequential quadratic programming (SQP).

To define a set of VoS variables a grid is superimposed on the design space, where the design variables become the fraction of each cell in this grid that is considered to consist of solid material, as shown in figure 1. This parameterisation procedure provides intuitive handling of topology change without explicit control of it, allowing flexibility while maintaining smooth control close to topology changes.

The capability of the RSVS parametrisation has been shown previously on aerodynamic shape and topology cases [56, 63]. A hierarchical approach to RSVS design variables was successfully implemented allowing the ex-

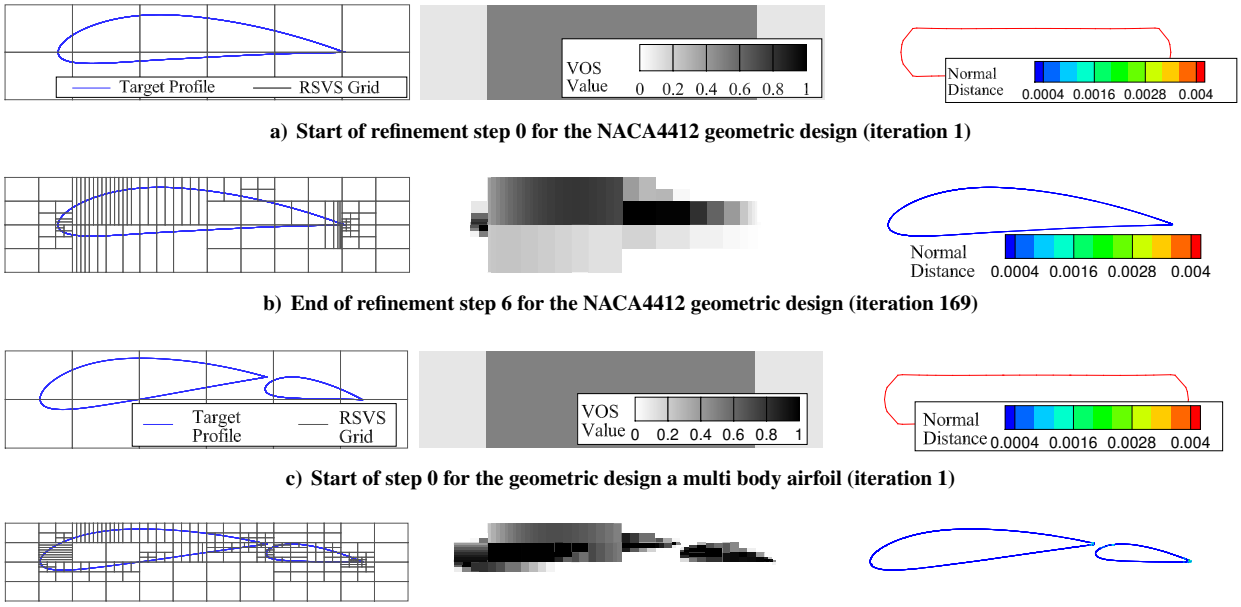

a) Start of refinement step 0 for the NACA4412 geometric design (iteration 1)

b) End of refinement step 6 for the NACA4412 geometric design (iteration 169)

c) Start of step 0 for the geometric design a multi body airfoil (iteration 1)

d) End of refinement step 8 for the geometric design a multi body airfoil (iteration 136)

Figure 3. Geometric recovery of a NACA4412 and a multi-body airfoil using up to 8 refinement steps starting from the same geometry; with the RSVS grid and the target profile (left), the VOS values for the geometry (centre) and the corresponding profile coloured according to its normal distance to the target profile (right) at the first and final iterations.

ploration of many optimisation cases without any change to the starting position of the optimisation framework [63]. This approach allows the geometric recovery of objects of arbitrary topology, this is shown in figure 3 for a multi-body aerofoil.

IV. Structural Topology Optimisation Framework

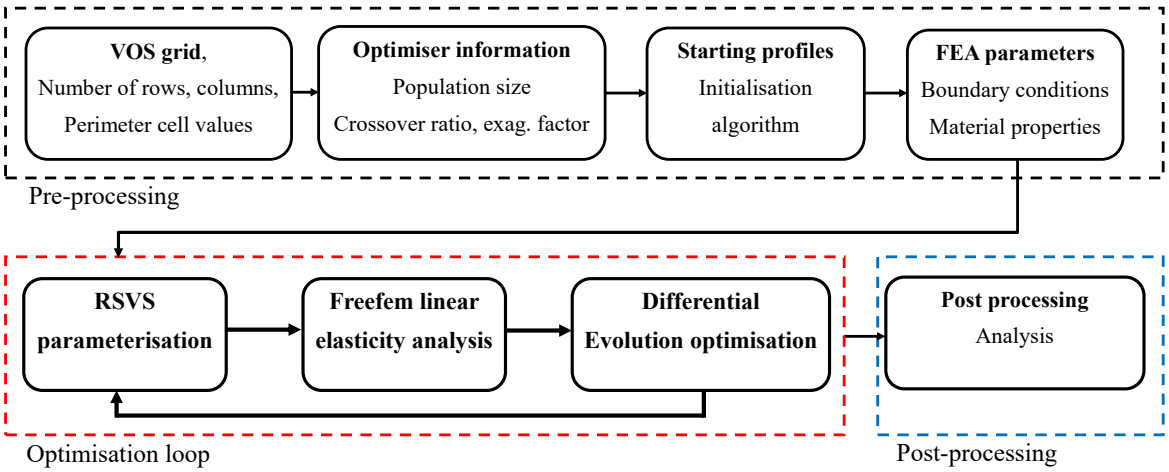

Figure 4. Flow chart showing the process followed for each test case.

A. Optimisers

The RSVS parameterisation is integrated in an optimisation framework which supports gradient-based and agent-based optimisers. This optimisation framework uses the volumes of the VoS cells as design variables, which are translated into geometry changes by the RSVS process.

Differential evolution is a heuristic global optimisation method proposed by Storn and Price [65], and was selected due to its robustness and ease of implementation both in serial and parallel. Unlike other heuristic methods it requires few internal parameters and has shown good results on a range of applications [66], notably for constrained optimization cases.

B. Finite Element Analysis Solver

An FEA solver was required for the evaluation of structural objective functions. FreeFem++ [67] is an open source partial differential equation solver run via a C++ style code and can be used to solve different types of finite element problems in two and three dimensions. This software has been previously used to write a density-based, and a level-set based structural optimisation framework [68]. Freefem was chosen for this task due to its simplicity, user-friendly formulation and previous use in structural optimisation.

Linear elasticity analysis was run via Lame's system of elasticity [67]. As all the problems considered are two-dimensional, plane stress conditions were assumed, and FreeFem's internal meshing procedures used. Freefem also facilitated mesh regulation via the 'adaptmesh' command, which allowed the original (potentially low quality) mesh to be re-meshed for specific target properties, including maximum and minimum element size. This means unevenly distributed coordinates can be converted into a regular mesh of the desired size. The left images of Figure 5 show an example original mesh alongside the corresponding improved mesh.

In Figure 5, the third figure from the left shows the local deflection difference between the regulated and unregulated mesh as a proportion of the maximum deflection. This can be seen to vary across the shape, with the largest difference in the region of 10^{-3} of the overall values. A mesh convergence study was performed and led to the choice of a mesh density between 3000 and 10000 vertices. Analysis was needed to ensure the mesh number was suitable for the optimisation process, and to ensure any numerical errors were suitably low. The far right graphic of Figure 5 shows the convergence of maximum deflection against mesh number.

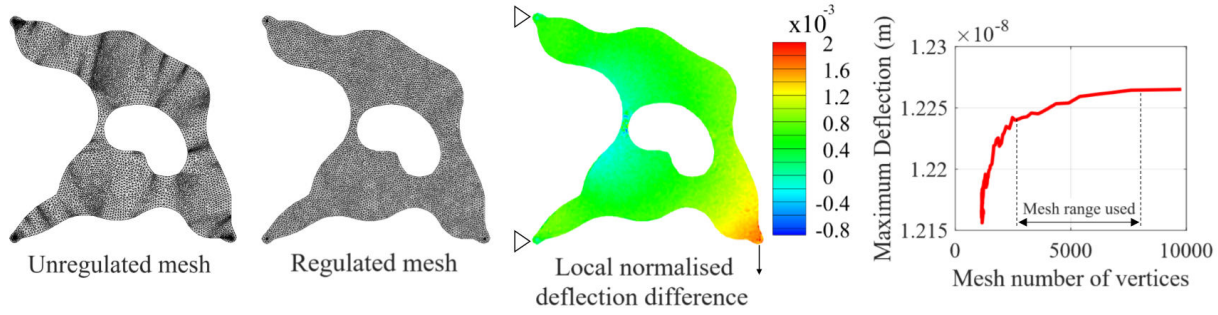

Figure 5. Mesh impact study. Sub-figures from left to right: unregulated mesh; regulated mesh; Local deflection comparison between meshes; Convergence of maximum deflection against mesh number of vertices.

C. Constraints

Valid RSVS parameter values need to be between 0 and 1 in each cell of the parameter grid, but optimisation algorithms can cause parameters to leave this range. If a parameter value is above one, the amount above one spills over to its neighbouring RSVS cells, and the value is set to one. The same process for parameters below zero takes place; these parameters absorb volume from their neighbours. This formulation gives an optimiser good control of the geometries, resulting in the smooth movement of boundaries across grid spaces, and therefore encouraging design space exploration.

Structural topology optimisation presents an important feasibility issue. To carry the load paths, one shape must connect the point of force with the boundary conditions. If not, the geometry will either be significantly inferior, or impossible to test. The issue was dealt with here using a 'death penalty'; if the object cannot carry the load, the objective function returned for the geometry is set to an extremely high value, meaning this geometry will not progress forward. Such a method works well for differential evolution, which exhibits a tournament selection process (the best shape goes forward), and uses no gradient information.

A maximum volume constraint was needed to ensure the design space would not fill with solid. The formulation of VoS enables a straight-forward way of handling this: the sum of the VoS parameters is directly proportional to the volume or area of the geometry produced. If the trialled VoS data from the optimiser warrants too great a volume, the values are all scaled down to a point where this is not the case. Across the whole design space only a small amount of scaling is usually needed.

Symmetry in optimisation can be used to reduce the dimensionality of the problem, reducing the number of iterations required for convergence. Symmetry was applied in the RSVS method through the parameter values. Every iteration, before the parameterisation, the parameters on one side of the line of symmetry would be mirrored on the other side.

D. Boundary Conditions and Design Space Specification

For the optimisation process to work as desired, the objective function must be extracted from each population member in a standardised way. This is to ensure the variation in objective function across different geometries is purely due to the structural performance of each geometry, based on the design variables only. Therefore, the positions of the boundary conditions (including forces) need to be standardised.

Figure 6 shows how this is achieved in RSVS structural optimisation. There exists an outer perimeter of design variables, which are constant throughout the whole optimisation process. The boundary conditions are applied in any VoS grid corner, which exists along the boundary between the active cells and the constrained perimeter cells. The point where this is applied is referred to as the boundary condition point. Cells in contact of these points are constrained to always have a small volume fraction, forcing the geometry to always be built around the force and constraint application regions. This is done for all the boundary condition points, and ensures there is space for the boundary conditions to be applied in the same place. The boundary conditions are applied to small circular borders placed at the exact points desired. The parameter numbers quoted in this work are referring to the active RSVS cells, so the VoS grid in figure 6 would be referred to as a 9 parameter VoS grid.

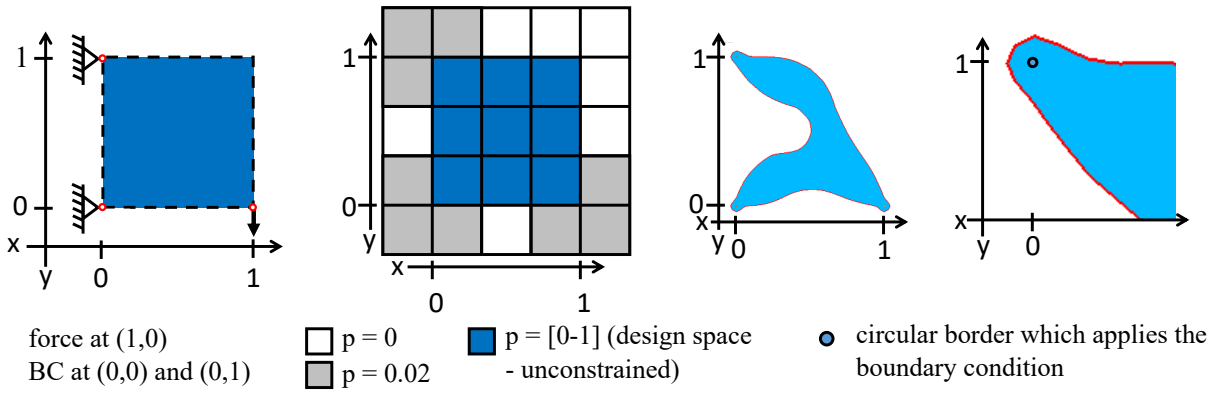

Figure 6. Demonstration of the application of boundary conditions to a 9 parameter problem. p is the VOS value.

E. Solution Comparison - SIMP Method and Border Extraction

To quantitatively benchmark the RSVS parameterisation a SIMP method, run in MATLAB, was also applied [1]. This code was developed by Sigmund and was intended to demonstrate the simplicity and versatility of SIMP, and spark interest in topology optimisation. The method produces a grey-scale image, with black corresponding to solid, and white to void. While the grey-scale images can be used to compare a topology with those found, an objective function value was needed for a quantitative comparison. This meant the grey-scale solution needed to be converted into coordinate profiles. The process for converting the given grey-scale solution, into a geometry comparable with those obtained through RSVS, is shown in Figure 7.

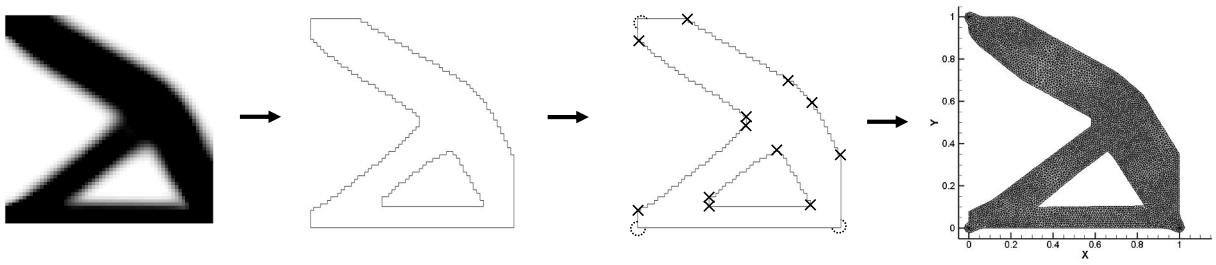

Figure 7. Process of extracting coordinates from the SIMP method grey-scale image.

First the outline of the grey-scale image was extracted using a MATLAB script. This jagged outline was found to perform badly with regard to the objective function. To remove the jagged edges produced by SIMP and compare the topological performance of the geometries like-for-like with the RSVS method the coordinates of the edges and curves of SIMP output were extracted and these coordinates connected with straight lines. For the corner pieces, the exact corner coordinates from the RSVS solution that the SIMP solution is to be compared to, are added. This was vital for fair comparisons, because the corner pieces affect structural performance.

Unfortunately this process is not perfect, due to the resolution of the SIMP grey-scales created, there are difficulties representing curves and translating those curves from the jagged outline produced. Reading coordinates of those jagged outlines then results in straight lines. As shown from Figure 7, the grey-scale on the left attempts to make a curve in certain places such as the top of the internal triangle, and the middle of the left side of the structure. These curves are lost in the jagged outline, and therefore are not seen in the output on the right. This will disadvantage the final SIMP objective functions. Density issues such as these are one of the main drawbacks of homogenisation methods such as SIMP, so the crisp borders produced by RSVS can be seen to give RSVS a fair advantage. This does present a possible use case in current STO frameworks for the RSVS as an automatic method for interpreting SIMP results. While the RSVS's formulation is not explicitly parameterised, the generated curves are non uniform rational B-splines (NURBS) a common class of shapes used in modelling. This means the RSVS allows the construction of

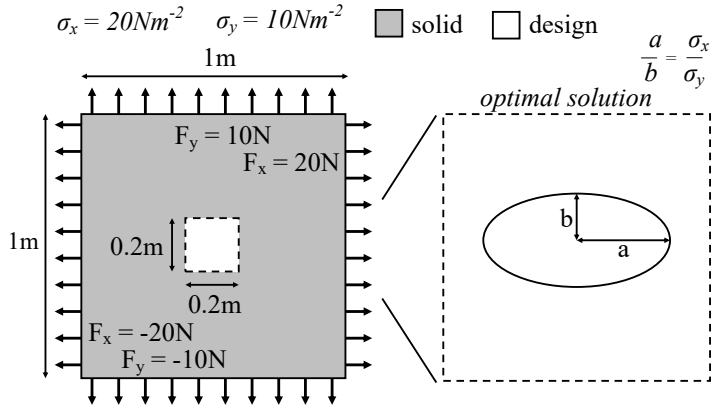

Figure 8. Problem definition and analytical solution of the hole in a bi-axial stress field.

profiles into NURBS of the correct topology which can then be used to produce a manufacturable models.

In figure 7, the far right image closely resembles those found by other methods. For example, geometries very similar to this (for the same problem), have been found from level-set methods [69–71], a homogenisation method [72], and a stochastic method [73]. This means there can be confidence in the SIMP method and used as benchmark, meaning the RSVS solutions can be quantitatively benchmarked.

V. Results

Six cases are presented, each highlighting a different feature of the RSVS parameterisation. The first example looks at the optimisation of a hold in bi-axial stress-field, it is a problem with similarities to aerodynamics. The next four cases study two cantilever beam and two MBB beam topology optimisation cases, and are presented in order of increasing size of the design space. Design variable refinement is used to progressively improve to the resolution of the RSVS parameterisation.

A. Hole in a Bi-axial Stress Field

Here a structural shape optimisation case is presented. The problem is as follows: a flat plate with a hole in, of theoretically infinite height and width, under a biaxial stress field, i.e. internal horizontal tension σ_x, and internal vertical tension σ_y. The plate is thin enough to assume plane stress conditions. The objective is to minimise the maximum von Mises stress divided by σ_x. The analytical solution to this problem is presented by Kristensen et Madsen [75] and the solution consists of an ellipse, with the semi-major axis a, over semi-minor axis b, equal to $\frac{\sigma_x}{\sigma_y}$, and in this example achieves an 'analytical' optimum of 1.5; the same geometry placed into the FE evaluation stage of the framework will be referred to as the 'numerical optimum'. Figure 9 shows the problem and optimal solution, and Equation 2 describes the optimisation problem. This problem can be seen as a bridging case between the ASO already carried out using RSVS, and structural topology optimisation.

$$\begin{aligned} \min \quad & \frac{max(\sigma_{VM})}{\sigma_x} \\ \text{s. t. } & A > 8 \times 10^{-3} \end{aligned} \tag{2}$$

The DE optimiser used a Latin Hypercube sample [76] randomised starting population and the minimum area of any matter removed was constrained to be $8\text{x}10^{-3}$ or above; this was needed to ensure a hole was present. Figure 9b shows a perfect ellipse with $\frac{a}{b} = 2$ (the analytical optimum). As the model has finite dimensions, smaller shapes score marginally better objective functions; however far more gain is to be found from producing a larger shape which closely resembles the desired ellipse, rather than a smaller but inferior shape. As the ellipse size decreases, the objective function output tends towards 1.5, the analytical optimum.

The ellipse designed by the optimiser resembles closely the analytical optimum, validating the optimisation framework. It is however slightly too large and too tall compared to the analytically predicted optimum, highlighting the

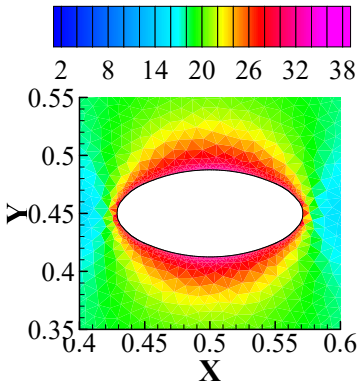

a) Optimisation solution, Ellipse volume = 8.25×10^{-3}, Max VM stress = 33.74, OF = 1.69.

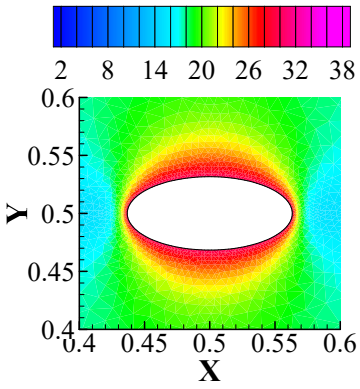

b) Numerical optimum, Ellipse volume = 8×10^{-3}. Max VM stress = 30.44, OF = 1.52.

Figure 9. Problem definition alongside von Mises stress plots (Nm^{-2}) of the found solution and numerical optimum.

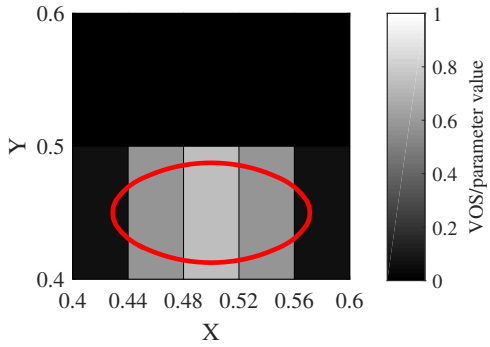

a) Parameter values of the found solution.

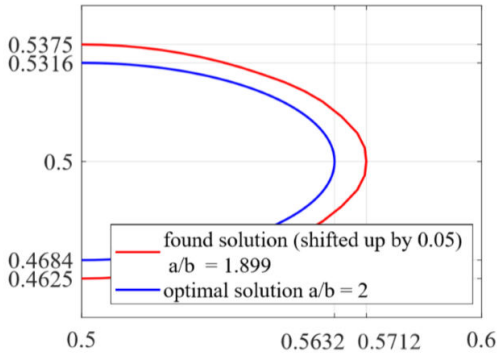

b) Shape comparison.

Figure 10. Parameter values and convergence history.

challenge of achieving local convergence when using a stochastic optimiser. This is shown by figure 10b, and is what causes the greater stress in the solution, and the 9.8% difference in the objective function.

B. Structural Topology Optimisation Examples

The results in this section present solutions to more complex structural topology optimisation problems. Freefem was set-up to mimic material properties of aluminium: a Poisson ratio of 0.3, and a Young's modulus of 69GPa.The choice of these properties is essentially arbitrary, as long as they are kept constant. All cases are loaded with a single, vertical force of 7.85N, with the optimisation problem for all examples in this as:

$$\begin{aligned} &\min \delta_f \\ &\text{s.t. } V < 0.5 \end{aligned} \tag{3}$$

With δ_f the absolute deflection at the point of the force, and V the proportion of the design space filled with solid (volume fraction). The problem is to minimise the deflection at the point of force (proportional to compliance), whilst filling no more than 50% of the design space. Volume constraints are common practice in STO and are easily enforced by the RSVS before the geometry generation, making this a natural choice of test case.

For these more complex topology optimisation tests, an initialisation algorithm was needed that had greater physical meaning regarding structural behaviour. Starting with a Latin Hypercube randomised starting population resulted in very poor results. This was due to the feasibility criteria described earlier. The majority of the starting profiles would not connect the boundary conditions. For each problem, there would be a most probable geometry to connect these.

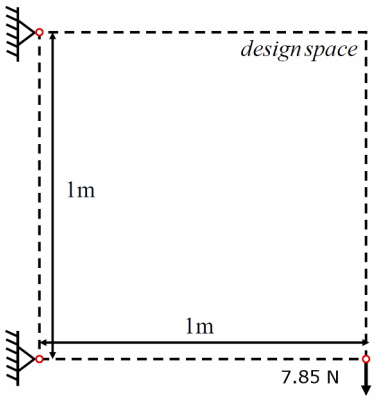

a) Problem definition.

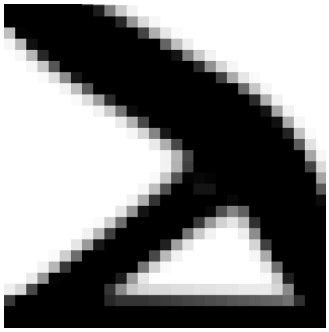

b) Example 1: Raw grey-scale SIMP solution.

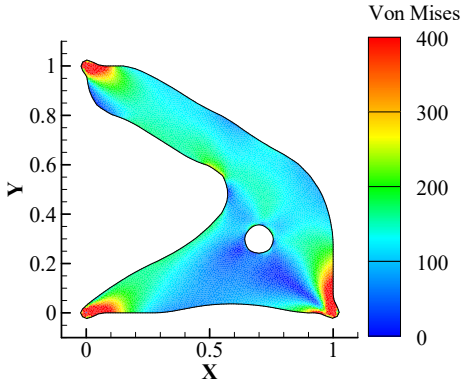

c) RSVS found solution volume = 0.4997, OF = 7.56e-9.

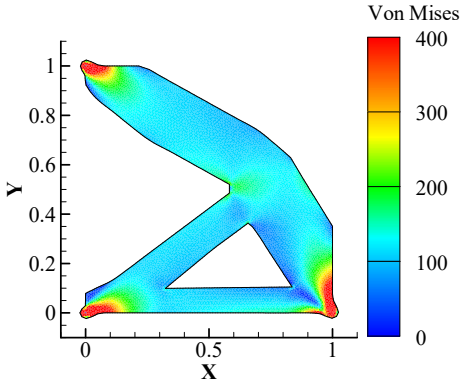

d) SIMP smoothed solution, volume = 0.4994, OF = 7.36e-9.

Figure 11. Problem definition and raw SIMP solution. Von Mises (Nm^{-2}) plots of the RSVS solution and smoothed SIMP solution. The RSVS solution has a 2.69% higher objective function.

As the process progressed more profiles would reach this geometry, and the process would prematurely converge on a local minimum. This meant the design space was not explored.

Hence, a starting population was required with all profiles meeting the feasibility criteria, but with these profiles distributed as randomly as possible across the design space. Using the parameters, each profile was built up from nothing via rows and columns of randomised position, length and thickness. When a parameter array was predicted to result in a profile connecting all the boundary conditions, it was given a position in the starting population. If a parameter array went above the volume constraint, the process would restart. The parameter arrays were also checked to ensure they were sufficiently different from previous arrays. This whole process could be done via the parameters due to the local physical meaning the parameters have over the design space. The starting populations produced this way resulted in an optimisation start point which covered the feasible design space. Because these profiles satisfied the feasibility condition, the combinations of these profiles and most child profiles followed suit. This meant the process was able to explore the feasible design space efficiently.

1. Case 1: Bottom Loaded Cantilever Beam

Here a square cantilever beam is loaded in the bottom corner. A VoS grid with 25 active parameters is used, 5(x) by 5(y). The run lasted a total of 321 iterations. Convergence was deemed as the objective function had not changed by more than 0.1% during the last 80 iterations.

Figures 11c and 11d show the von Mises stress plots of the RSVS solution and SIMP solution. One can see the RSVS solution has been able to match the topology of the SIMP solution, and closely resemble the outline. The hole produced in the RSVS solution is in the right place, but is a circle as opposed to the more sophisticated and larger triangle in the SIMP solution. This area for the RSVS solution has a dark blue colour, meaning the stress is low here,

and material here is not being put to optimal use. On the other hand the SIMP solution has a more even stress field (more light blue), meaning it is making the most use of its material. It is likely to be this reason why the SIMP solution has a 3% lower objective function.

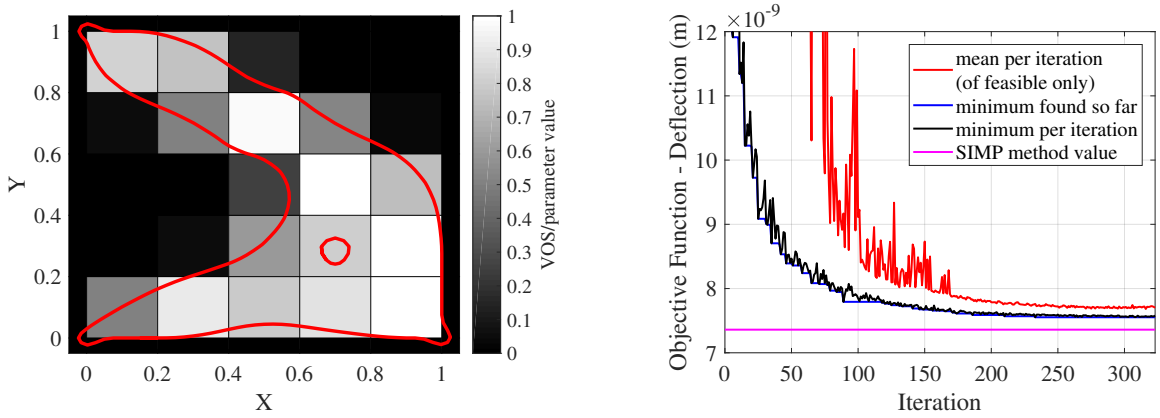

a) 25 parameters of the found solution. **b) Convergence history.**

Figure 12. Parameters and convergence history.

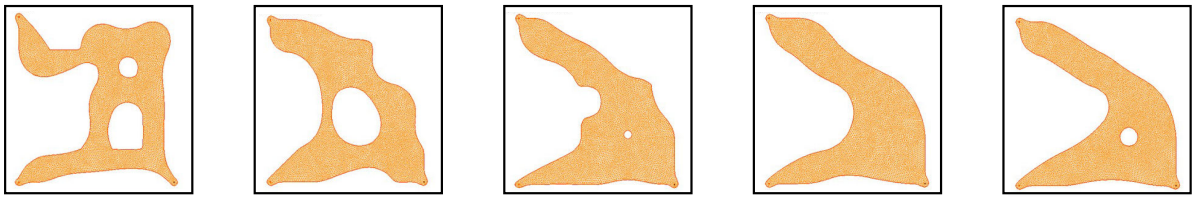

Best at iteration 1 **OF: 2.78e-8**

Best at iteration 40 **OF: 8.70e-9**

Best at iteration 80 **OF: 7.97e-9**

Best at iteration 160 **OF: 7.66e-9**

Best at iteration 323 **OF: 7.56e-9**

Figure 13. Evolution history of the bottom loaded cantilever.

2. *Case 1 revisited: Higher Fidelity Result*

This case was run again with an 8x8 grid. The dimensions and boundary conditions are identical to those from Example 1. Figure 14 shows the RSVS solution to the problem on an 8x8 grid. This is clearly closer to the SIMP solution, and scores a much closer objective function value. This result is not yet converged so would likely be improved given more runtime. There is also the option to use local optimisation to improve this result. This demonstrates that RSVS creates a better solution given more flexibility. The internal hole is spread over a larger number of VoS cells, so can take the form of a more complex geometric shape.

The result was created starting with an 8x8 grid from scratch. There is the option to start with a 4x4 grid and split the grid dynamically into an 8x8 grid. This process of dynamic refinement is explored in section C. For instance the external outline is sufficient in both the 5x5 and 8x8 solutions. The internal hole in the 5x5 solution does not cover enough VOS cells to take any form other than a circle. Splitting this VOS cell and certain cells around it would give RSVS the flexibility to shape the internal hole. This would be much more efficient than starting with a finer grid or splitting all the VOS cells, i.e. it keeps the parameter number compact.

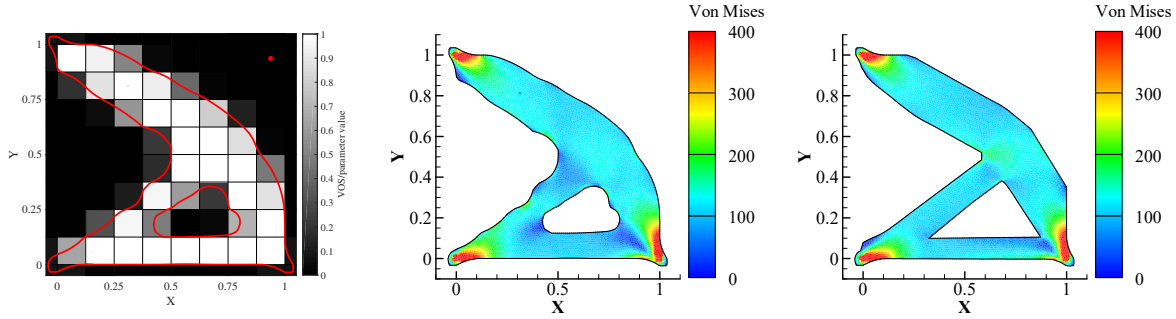

a) Parameter values used to create the solution above.

b) RSVS found solution volume = 0.4998, OF = 6.96e-9.

c) SIMP smoothed solution, volume = 0.4975, OF = 6.95e-9.

Figure 14. Von Mises (Nm^{-2}) plots of the RSVS solution and smoothed SIMP solution and parameter values used to create this solution. The RSVS solution has a 0.2% higher objective function.

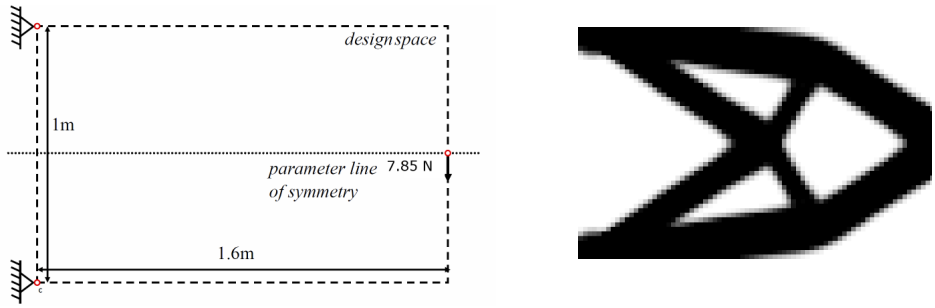

a) Problem definition.

b) Raw greyscale Simp solution.

Figure 15. Problem definition and raw SIMP solution.

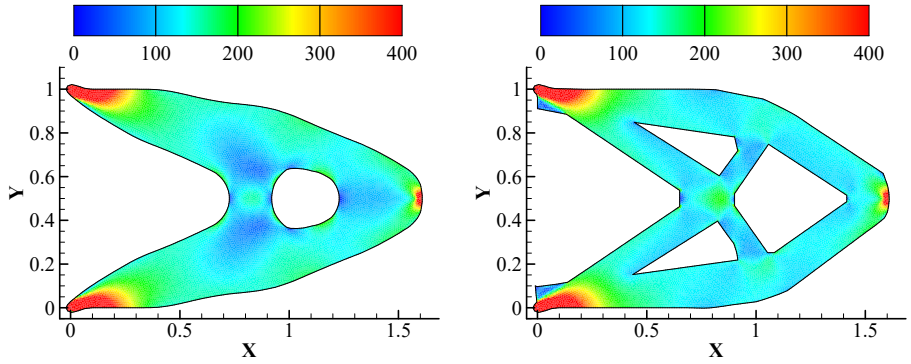

a) RSVS found solution, volume = 0.7985, OF = 1.45e-8.

b) SIMP smoothed solution, volume = 0.7961, OF = 1.40e-8.

Figure 16. Von Mises (Nm^{-2}) plots of the RSVS solution and smoothed SIMP solution. The RSVS solution has a 3.3% higher objective function.

3. *Case 2: Centrally Loaded Cantilever Beam*

Here, optimisation of a centrally loaded cantilever beam, with a 1.6 aspect ratio, was tested. A 24 active cell grid, 6(x) by 4(y) was used, per half. Vertical symmetry was applied through the centre. The RSVS solution is likely disadvantaged by only having one hole, as opposed to three of the SIMP solution. However, the smooth outer border of the RSVS solution results in a close objective function (only 3% higher). This result currently shows that the RSVS framework is able to create a sufficient solution given its VOS resolution. Local grid refinement could be used to improve this results. By increasing the resolution of the VOS grid in certain places, RSVS will have more flexibility to create smaller internal holes so its solution is closer to that of SIMP.

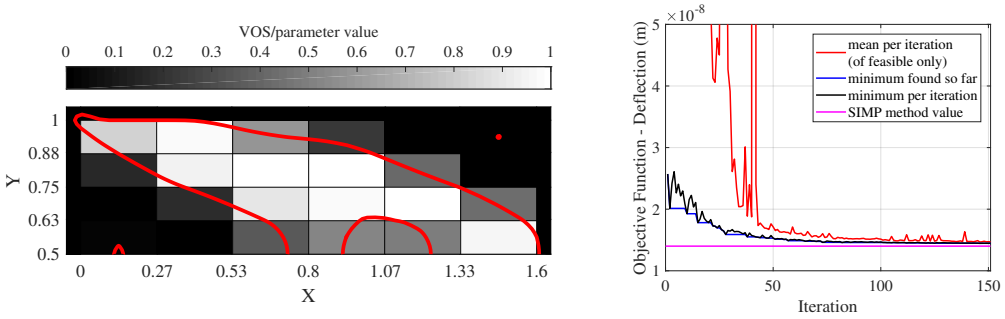

a) The 24 parameters of the final solution. **b) Convergence History.**

Figure 17. Graphic showing the parameter values and convergence history.

4. *Case 3: MBB Beam*

Optimisation of a centrally loaded beam, with an aspect ratio of 4 is presented here. This is a common benchmark case in the field of structural optimisation, and is commonly known as to as the Messerschmidt-Blkow-Blohm or 'MBB' beam. Here, a 25 cell active grid is used, 5(x) by 5(y), per half. Horizontal symmetry is applied through the centre [1, 77, 78].

RSVS with this fidelity would not be able to create SIMP's truss-based structure, due to the difficulty in extracting sharp triangles. However, the optimiser was able to find another suitable layout, an archway shape. The smoothness of this meant a lower objective function than the truss-like structure from the SIMP method. The top half of the solution, the sections in compression, have created an archway which have good structural behaviour in compression, and can be found in many practical examples, including Roman architecture. For example, the RSVS solution here has close resemblance with the Cangas de Onis bridge in Spain. The archway on the bridge does not need a lower beam, as the forces are transferred into the ground. In the MBB beam problem, the forces are transferred into the beam along the bottom, which in the RSVS solution has been made using the bottom row of design variables. This beam transfers the forces to the boundary conditions.

The advantage of the RSVS solution can be seen in Figure 20a and 20b. The RSVS solution shows a more even distribution of von Mises stress, with lots of material around the 125Nm^{-2} mark (light blue). The SIMP solution has more force around the 200Nm^{-2} mark (green), and compensates this with lots of other material around 50Nm^{-2} (dark blue). Hence the SIMP solution has a less even distribution of force, which translates to a higher deflection.

5. *Case 4: Stretched MBB Beam*

Here an MBB beam with an aspect ratio of 8 is presented. For clarity, this is referred to here as the stretched MBB beam. A 21 cell active grid is used, 7(x) by 3(y), per half. Horizontal symmetry is applied through the centre.

It is clear that the RSVS solution does not perform as well as in the previous cases. This can be seen from the uneven distribution of stress in Figure 25b. Figure 25a shows the SIMP layout is able to carry the forces through a series of diagonal struts, which follow the load path. The RSVS layout has only made vertical columns; these impede the natural load path. This is shown by the diagonal 300-400Nm^{-2} (yellow-red) lines of stress in Figure 25b.

The minimum per iteration of figure 26b implies the profile has converged. The erratic iteration mean is due to the thinning of the shape by the boundary condition as shown by the left corner in figure 26a. On some profiles this border becomes extremely thin, resulting in extremely high objective function values. Although it appears the

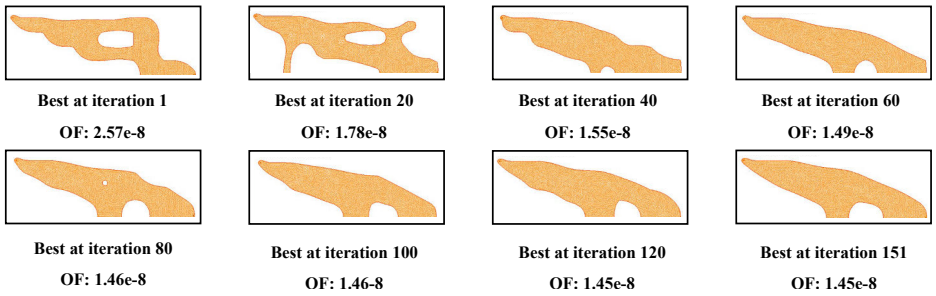

Figure 18. Evolution history of the centrally loaded cantilever beam.

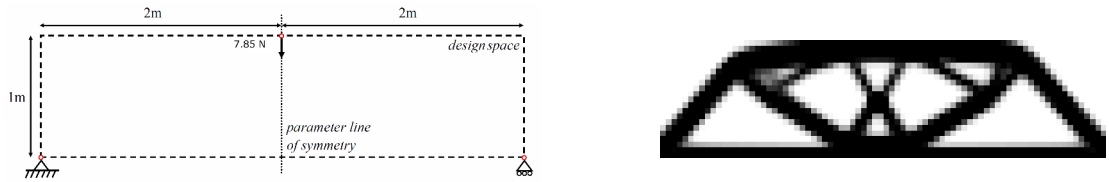

a) Problem definition. **b) Raw greyscale SIMP solution.**

Figure 19. Problem definition and raw SIMP solution for the MBB beam.

optimiser would not change from this topology in future, this process would likely need to be continued for complete convergence. The transverse movement of the outer border is likely due to the lack of fidelity in the y-axis. Figure 26a shows only 3 parameters are used in the y-direction. More cells are needed to produce a straight beam along the bottom, give the shape a more consistent upper border, and shape the internal holes into triangles. This example highlights the importance of choosing the right VoS grid for the problem.

C. Investigation of VOS Grid Refinement

The primary issue from the previous results appears to be the definition of small enough internal holes. Here grid refinement is explored as a possible option to alleviate this issue. Grid refinement involves subdividing cells in certain VOS grid spaces to create a larger number of smaller cells in that space. This gives more local flexibility in the geometries represented.

The result here show the centrally loaded cantilever beam. This case was chosen for grid refinement because as shown in Example 2, the shape of the hole in the RSVS solution is tending towards that of the hole in the SIMP solution, but lacks sharpness in its definition.

To trial grid refinement, an initial 4(x) by 8(y) VoS grid was used, with a horizontal line of symmetry as applied

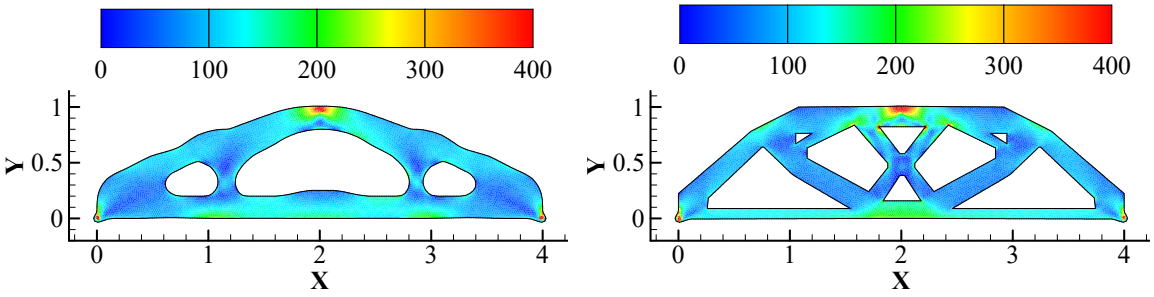

a) RSVS found solution, volume = 1.995, OF = 1.36e-8. **b) SIMP smoothed solution, volume = 1.9942, OF = 1.48e-8.**

Figure 20. Von Mises (Nm^{-2}) plots of the RSVS solution and smoothed SIMP solution. The RSVS solution has a 8.1% lower objective function.

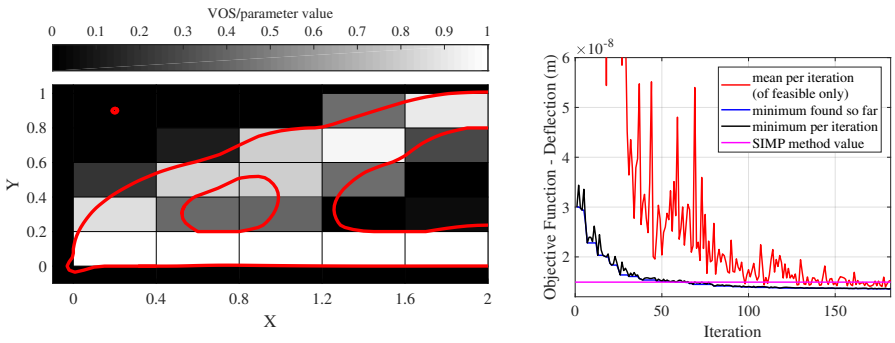

a) The 25 parameters of the final solution. **b) Convergence History.**

Figure 21. Graphic showing the parameter values and convergence history.

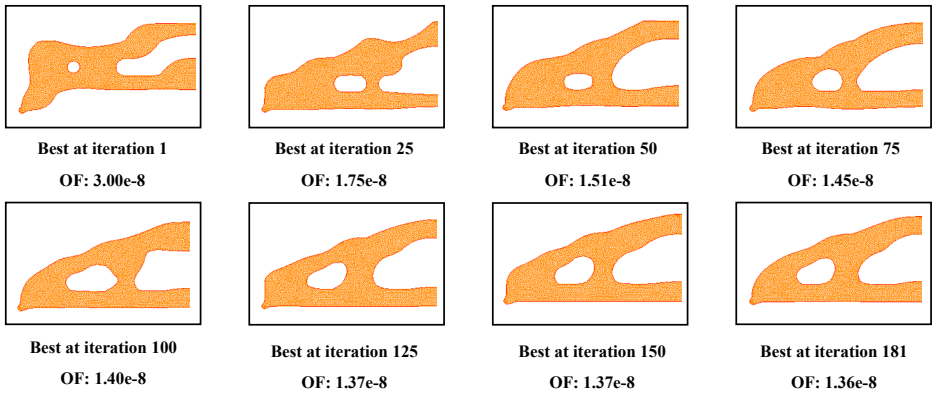

Figure 22. Evolution history of the MBB beam.

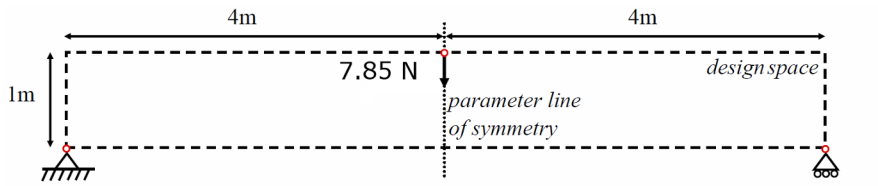

Figure 23. Problem definition for the long MBB beam.

Figure 24. Raw SIMP solution for the stretched MBB beam.

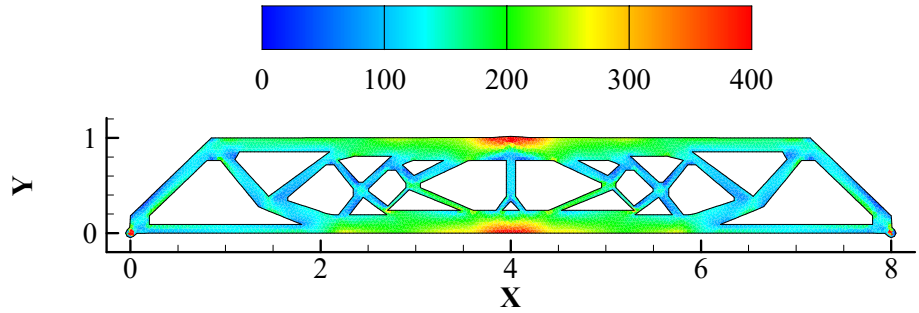

a) SIMP smoothed solution, volume = 3.9981, OF = 6.12e-8.

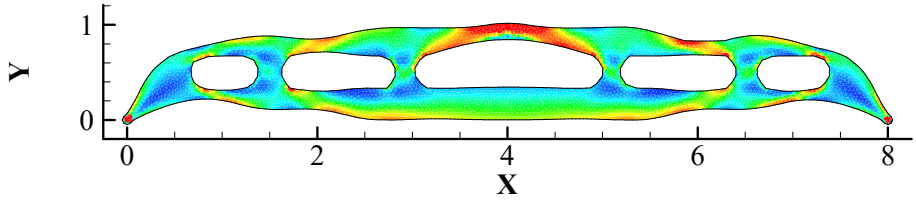

b) RSVS found solution, volume = 3.9995, OF = 8.33e-8.

Figure 25. Von Mises (Nm^{-2}) plots of the RSVS solution and smoothed SIMP solution. The RSVS solution has a 40% higher objective function.

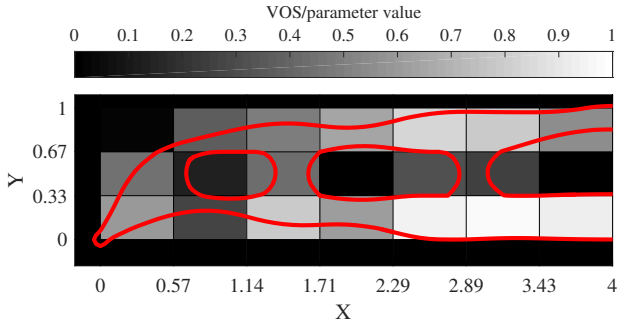

a) The 21 parameters of the final solution.

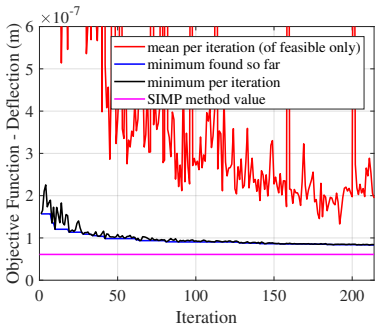

b) Convergence History.

Figure 26. Graphic showing the parameter values and convergence history.

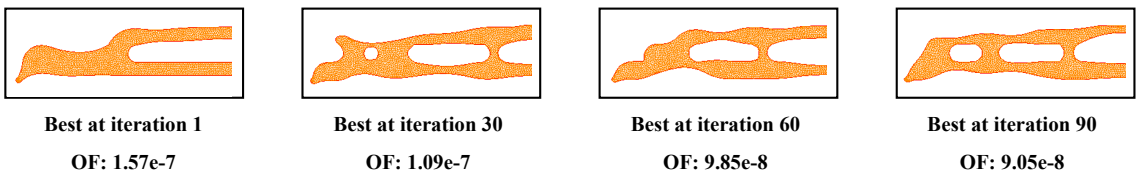

Best at iteration 1
OF: 1.57e-7

Best at iteration 30
OF: 1.09e-7

Best at iteration 60
OF: 9.85e-8

Best at iteration 90
OF: 9.05e-8

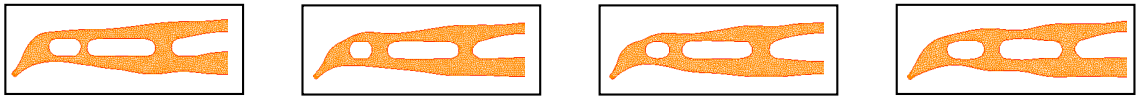

Best at iteration 124
OF: 9.05e-8

Best at iteration 150
OF: 8.64-8

Best at iteration 180
OF: 8.51e-8

Best at iteration 211
OF: 8.33e-8

Figure 27. Evolution history of the stretched MBB beam.

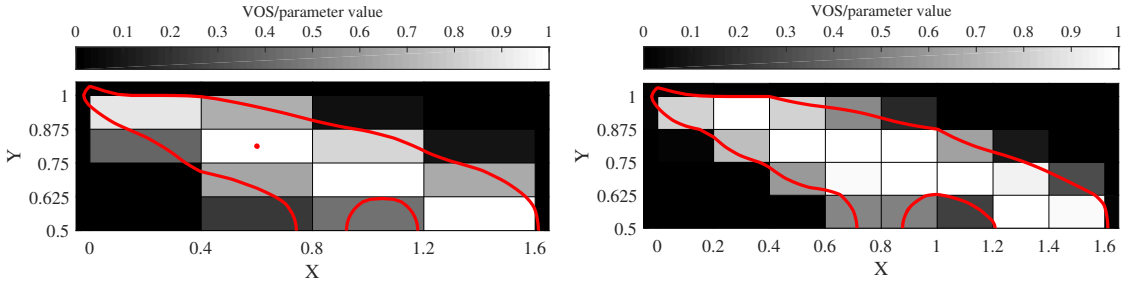

a) Initial 16 active parameters. **b) Refined 32 active parameters.**

Figure 28. Solutions shown over parameter values for the initial solution on the original grid, and solution after refinement on the refined grid.

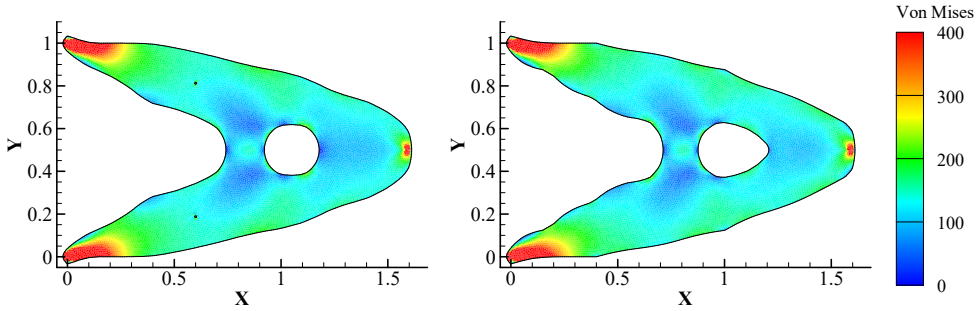

a) Solution from intial grid. OF: 3.9% higher than equivalent SIMP solution. **b) Solution from refined grid OF: 2.2% higher than equivalent SIMP solution.**

Figure 29. Von Mises stress (Nm^{-2}) plots of the initial and refined solution. The refined solution improves the objective function by 1.7% against the equivalent SIMP solution.

in Example 2. The problem definition is identical to that in Figure 15a. The initial stage of optimisation was run for 95 iterations, at which point all members of the population were the same shape and a good solution had been found, but there was still some variance left in the borders of the population. This process resulted in the solution shown in Figure 28a. The grid was then refined; all active cells were split horizontally into two. There was no reseeding; all solutions in the population were interpolated onto the new VOS grid. It was for this reason the initial stage was stopped before complete convergence, as the differential evolution optimiser needs variance in a population to progress. The process was run for another 100 iterations, at which point the solution shown in Figure 28b had been produced. It can be seen that the border of the refined solution is jagged and not optimal. This is due to the process not converging completely, and the refinement likely happening after too much convergence, i.e. the optimiser not having enough variance in the population to morph the boundary of the shape.

The main conclusion to draw from this is the sharpening of the internal hole. The hole on the initial solution is circular, whereas the hole on the refined grid is triangular, which is a lot closer to the diamond-shaped hole from the SIMP solution. Figure 28a shows that 2 cells (1 per half) are used to define the hole from the initial solution. This becomes 10 (5 per half) after the refinement, as the hole is able to grow into other now unused cells. Therefore the sharp point on the right of the internal hole can be defined. This result shows that grid refinement is able to sharpen an internal hole, and therefore help alleviate the main drawback to RSVS-based structural optimisation.

Here only simple restart procedure was envisaged where the VOS design variables on a the initial grid are translated into VOS for a finer set of design variables. The optimiser then continued with a new set of design variables but the same population. This did not prove sufficient as the DE algorithm was unable to exploit the new design space to find much better designs has had been observed for aerodynamic problems [79]. Some attempts at re-seeding the design space to provide diversity in the new cells was carried out but this led to convergence no better than starting from finer grid from scratch. This highlights the specific challenge of design variable refinement with agent based optimisers where diversity and quality of geometries needs to be balanced with the number of objective function calls that will be

required for the population to converge. To fully evaluate the potential of refinement, integration with gradient based optimisation and a mechanism for the introduction of holes is required.

This difficulty might be due in part to the study of volume constrained, deflection minimisation problems where the reseeding of the design space needs to balance introduction of new topologies and maintaining an area close to the constraint value. Cases of VOS minimisation under stress constraint might be more amenable to reseeding as the volume constraint would not need to be maintained.

VI. Conclusion

A framework has been developed to use the RSVS parameterisation in structural optimisation. After validating this framework in a straight forward structural optimisation case, RSVS has been trialled in four structural topology optimisation cases, all using 25 parameters or less. The final solutions of these cases were compared with those from a low fidelity homogenisation method. For two cantilever beam tests, the RSVS solution produced objective functions to within 3% of those of the homogenisation method. A recent publication by Valdez et al. [74] proposes standardisations of the benchmarking of 2 dimensional topology optimisation problems, future studies will look into those cases to allow quantitative comparison with other methods.

The results demonstrate that the RSVS parameterisation is able to create smooth solutions that follow internal load paths. It is also able to explore different topologies, and converge on a suitable shape, resulting in the RSVS process correctly distributing material. The use of refinement did not prove as beneficial as previous evidence suggested [13, 14, 63]. Integration of a gradient based process with topological derivatives could allow the larger number of design variables introduced by refinement to be exploited more efficiently.

The work here is intended to answer the question of whether RSVS parameterisation can be integrated into structural optimisation, and therefore be used in multidisciplinary optimisation. The results so far show RSVS has potential in structural optimisation, and therefore could be used in multidisciplinary optimisation. For further studies of the RSVS in STO it could be interesting to define the restricted snake used by the RSVS directly on a constant analysis mesh, this would bring this method fundamentally closer to some LSM implementations. The work presented here has shown that the RSVS could be used in structural and aerodynamic contexts: this opens the possibility of a general aero-structural optimisation framework using a single parameterisation.

Acknowledgements

This work was carried out using the computational facilities of the Advanced Computing Research Centre, University of Bristol - http://www.bris.ac.uk/acrc/. Funding: This work was supported by the EPSRC Research Council UK and the University of Bristol through DTP grant EP/M507994/1. All the data needed to support the conclusions of this article are presented in the paper.

References

[1] Sigmund, O., "A 99 line topology optimization code written in Matlab," *Structural and Multidisciplinary Optimization*, Vol. 21, No. 2, Apr 2001, pp. 120–127.

[2] Aage, N., Andreassen, E., Lazarov, B. S., and Sigmund, O., "Giga-voxel computational morphogenesis for structural design," *Nature*, Vol. 550, No. 7674, oct 2017, pp. 84–86.

[3] Kenway, G. K., Burdette, D. A., and Martins, J., "Multipoint Aerodynamic Shape Optimization Investigations of the Common Research Model Wing," *53rd AIAA Aerospace Sciences Meeting*, AIAA SciTech, American Institute of Aeronautics and Astronautics, Reston, Virginia, jan 2015.

[4] Burdette, D. A. and Martins, J. R., "Design of a transonic wing with an adaptive morphing trailing edge via aerostructural optimization," *Aerospace Science and Technology*, Vol. 81, oct 2018, pp. 192–203.

[5] Lyu, Z., Kenway, G. K. W., and Martins, J. R. R. A., "Aerodynamic Shape Optimization Investigations of the Common Research Model Wing Benchmark," *AIAA Journal*, Vol. 53, No. 4, apr 2015, pp. 968–985.

[6] Payot, A. D. J., Rendall, T. C. S., and Allen, C. B., "Restricted Snakes: a Flexible Topology Parameterisation Method for Aerodynamic Optimisation," *55th AIAA Aerospace Sciences Meeting*, Vol. 8, Jan 2017, pp. 42–51.

[7] Payot, A. D. J., Rendall, T. C. S., and Allen, C. B., "Mixing and Refinement of Design Variables for Geometry and Topology Optimization in Aerodynamics," *35th AIAA Applied Aerodynamics Conference*, 2017.

[8] Masters, D. A., Taylor, N. J., Rendall, T. C. S., and Allen, C. B., "Multilevel Subdivision Parameterization Scheme for Aerodynamic Shape Optimization," *AIAA Journal*, Vol. 55, No. 10, oct 2017, pp. 3288–3303.

[9] Masters, D. A., Taylor, N. J., Rendall, T., and Allen, C. B., "A Locally Adaptive Subdivision Parameterisation Scheme for Aerodynamic Shape Optimisation," *34th AIAA Applied Aerodynamics Conference*, American Institute of Aeronautics and Astronautics, Reston, Virginia, jun 2016, p. 3866.

[10] Anderson, G. R. and Aftosmis, M. J., "Adaptive Shape Control for Aerodynamic Design," *56th AIAA/ASCE/AHS/ASC Structures, Structural Dynamics, and Materials Conference*, American Institute of Aeronautics and Astronautics, Reston, Virginia, jan 2015.

[11] Anderson, G. R., Nemec, M., and Aftosmis, M. J., "Aerodynamic Shape Optimization Benchmarks with Error Control and Automatic Parameterization," *53rd AIAA Aerospace Sciences Meeting*, American Institute of Aeronautics and Astronautics, Reston, Virginia, jan 2015.

[12] Maute, K. and Ramm, E., "Adaptive topology optimization," *Structural Optimization*, Vol. 10, No. 2, oct 1995, pp. 100–112.

[13] Kim, I. Y. and De Weck, O. L., "Variable chromosome length genetic algorithm for progressive refinement in topology optimization," *Structural and Multidisciplinary Optimization*, Vol. 29, No. 6, 2005, pp. 445–456.

[14] Bandara, K., Rüberg, T., and Cirak, F., "Shape optimisation with multiresolution subdivision surfaces and immersed finite elements," *Computer Methods in Applied Mechanics and Engineering*, Vol. 300, mar 2016, pp. 510–539.

[15] Kedward, L., Payot, A. D., Rendall, T., and Allen, C. B., "Efficient Multi-Resolution Approaches for Exploration of External Aerodynamic Shape and Topology," *2018 Applied Aerodynamics Conference*, American Institute of Aeronautics and Astronautics, Reston, Virginia, jun 2018.

[16] M.C.E., A. M., "LVIII. The limits of economy of material in frame-structures," *The London, Edinburgh, and Dublin Philosophical Magazine and Journal of Science*, Vol. 8, No. 47, 1904, pp. 589–597.

[17] Bendsø e, M. P. and Kikuchi, N., "Generating Optimal Topologies in Structural Design Using a Homogenization Method," *Comput. Methods Appl. Mech. Eng.*, Vol. 71, No. 2, Nov. 1988, pp. 197–224.

[18] Grihon, S., "A380 Weight Savings using Numerical Structural Optimisation," *AAAF Materials for Aerospace Applications 20th AAAF Colloquium, At Paris*, 2003.

[19] Hunter, E., "Alternate Detail Part Design and Analysis: Topology, Size, and Shape Optimization of CH-47 Chinook Underfloor Structure," *The Boeing Company*, 11 2006.

[20] Rozvany, G. I. N., "A critical review of established methods of structural topology optimization," *Structural and Multidisciplinary Optimization*, Vol. 37, No. 3, Jan 2009, pp. 217–237.

[21] Bendsøe, M. P., "Optimal shape design as a material distribution problem," *Structural optimization*, Vol. 1, No. 4, Dec 1989, pp. 193–202.

[22] Tanskanen, P., "The evolutionary structural optimization method: theoretical aspects," *Computer Methods in Applied Mechanics and Engineering*, Vol. 191, No. 47, 2002, pp. 5485 – 5498.

[23] van Dijk, N. P., Maute, K., Langelaar, M., and van Keulen, F., "Level-set methods for structural topology optimization: a review," *Structural and Multidisciplinary Optimization*, Vol. 48, No. 3, sep 2013, pp. 437–472.

[24] Eschenauer, H. A., Kobelev, V. V., and Schumacher, A., "Bubble method for topology and shape optimization of structures," *Structural optimization*, Vol. 8, No. 1, Aug 1994, pp. 42–51.

[25] Sigmund, O. and Maute, K., "Topology optimization approaches," *Structural and Multidisciplinary Optimization*, Vol. 48, No. 6, dec 2013, pp. 1031–1055.

[26] Gain, A. L. and Paulino, G. H., "A critical comparative assessment of differential equation-driven methods for structural topology optimization," *Structural and Multidisciplinary Optimization*, Vol. 48, No. 4, oct 2013, pp. 685–710.

[27] Allaire, G., Jouve, F., and Toader, A.-M., "Structural optimization using sensitivity analysis and a level-set method," *Journal of Computational Physics*, Vol. 194, No. 1, feb 2004, pp. 363–393.

[28] Nguyen, T. H., Paulino, G. H., Song, J., and Le, C. H., "A computational paradigm for multiresolution topology optimization (MTOP)," *Structural and Multidisciplinary Optimization*, Vol. 41, No. 4, apr 2010, pp. 525–539.

[29] Yamada, T., Izui, K., Nishiwaki, S., and Takezawa, A., "A topology optimization method based on the level set method incorporating a fictitious interface energy," *Computer Methods in Applied Mechanics and Engineering*, Vol. 199, No. 45-48, nov 2010, pp. 2876–2891.

[30] Deaton, J. D. and Grandhi, R. V., "A survey of structural and multidisciplinary continuum topology optimization: post 2000," *Struct Multidisc Optim*, Vol. 49, 2014, pp. 1–38.

[31] Aage, N., Poulsen, T. H., Gersborg-Hansen, A., and Sigmund, O., "Topology optimization of large scale stokes flow problems," *Structural and Multidisciplinary Optimization*, Vol. 35, No. 2, feb 2008, pp. 175–180.

[32] Kreissl, S., Pingen, G., Evgrafov, A., and Maute, K., "Topology optimization of flexible micro-fluidic devices," *Structural and Multidisciplinary Optimization*, Vol. 42, No. 4, oct 2010, pp. 495–516.

[33] Burman, E. and Hansbo, P., "Fictitious domain finite element methods using cut elements: II. A stabilized Nitsche method," *Applied Numerical Mathematics*, Vol. 62, No. 4, apr 2012, pp. 328–341.

[34] Villanueva, C. H. and Maute, K., "CutFEM topology optimization of 3D laminar incompressible flow problems," *Computer Methods in Applied Mechanics and Engineering*, Vol. 320, 2017, pp. 444–473.

[35] Deng, Y., Liu, Z., Zhang, P., Liu, Y., and Wu, Y., "Topology optimization of unsteady incompressible NavierStokes flows," *Journal of Computational Physics*, Vol. 230, No. 17, jul 2011, pp. 6688–6708.

[36] Kulfan, B. and Bussoletti, J., ""Fundamental" Parameteric Geometry Representations for Aircraft Component Shapes," *11th AIAA/ISSMO Multidisciplinary Analysis and Optimization Conference*, Vol. 1, American Institute of Aeronautics and Astronautics, Reston, Virigina, sep 2006, pp. 547–591.

[37] Sobieczky, H., *Parametric Airfoils and Wings*, chap. Parametric, Vieweg+Teubner Verlag, Wiesbaden, 1998, pp. 71–87.

[38] Hicks, R. M. and Henne, P. A., "Wing Design by Numerical Optimization," *Journal of Aircraft*, Vol. 15, No. 7, jul 1978, pp. 407–412.

[39] Gagnon, H. and Zingg, D. W., "Two-Level Free-Form and Axial Deformation for Exploratory Aerodynamic Shape Optimization," *AIAA Journal*, Vol. 53, No. 7, jul 2015, pp. 2015–2026.

[40] Poole, D. J., Allen, C. B., and Rendall, T. C. S., "Metric-Based Mathematical Derivation of Efficient Airfoil Design Variables," *AIAA Journal*, Vol. 53, No. 5, may 2015, pp. 1349–1361.

[41] Masters, D. A., Taylor, N. J., Rendall, T., and Allen, C. B., "Three-Dimensional Subdivision Parameterisation for Aerodynamic Shape Optimisation," *55th AIAA Aerospace Sciences Meeting*, , No. January, 2017, pp. 1–17.

[42] Kedward, L., Allen, C. B., and Rendall, T., "Gradient-Limiting Shape Control for Efficient Aerodynamic Optimisation," *2018 Applied Aerodynamics Conference*, American Institute of Aeronautics and Astronautics, Reston, Virginia, jun 2018, pp. 1–22.

[43] Masters, D. a., Taylor, N. J., Rendall, T. C. S., Allen, C. B., and Poole, D. J., "Geometric Comparison of Aerofoil Shape Parameterization Methods," *AIAA Journal*, Vol. 55, No. 5, may 2017, pp. 1575–1589.

[44] Masters, D. A., Poole, D. J., Taylor, N. J., Rendall, T. C. S., and Allen, C. B., "Influence of Shape Parameterization on a Benchmark Aerodynamic Optimization Problem," *Journal of Aircraft*, Vol. 54, No. 6, nov 2017, pp. 2242–2256.

[45] Hall, J., Poole, D., Rendall, T., and Allen, C., "Volumetric Shape Parameterisation for Combined Aerodynamic Geometry and Topology Optimisation," *AIAA paper AIAA2015-3354, Proceedings 16th AIAA/ISSMO Multidisciplinary Analysis and Optimization Conference*, 06 2015.

[46] Gill, P. E., Murray, W., and Saunders, M. a., "SNOPT: An SQP Algorithm for Large-Scale Constrained Optimization," *SIAM Journal on Optimization*, Vol. 12, No. 4, jan 2002, pp. 979–1006.

[47] Secco, N. R. and Martins, J. R. R. A., "RANS-Based Aerodynamic Shape Optimization of a Strut-Braced Wing with Overset Meshes," *Journal of Aircraft*, sep 2018, pp. 1–11.

[48] Streuber, G. and Zingg, D. W., "A Parametric Study of Multimodality in Aerodynamic Shape Optimization of Wings," *2018 Multidisciplinary Analysis and Optimization Conference*, American Institute of Aeronautics and Astronautics, Reston, Virginia, jun 2018, pp. 1–22.

[49] Shi-Dong, D. and Nadarajah, S., "Approximate Hessian for accelerated convergence of aerodynamic shape optimization problems in an adjoint-based framework," *Computers and Fluids*, Vol. 168, 2018, pp. 265–284.

[50] Pironneau, O., *Optimal Shape Design for Elliptic Systems*, 1983.

[51] Jameson, A., "Aerodynamic design via control theory," *Journal of Scientific Computing*, Vol. 3, No. 3, Sep 1988, pp. 233–260.

[52] Das, S. and Suganthan, P. N., "Differential Evolution: A Survey of the State-of-the-Art," *IEEE Transactions on Evolutionary Computation*, Vol. 15, No. 1, Feb 2011, pp. 4–31.

[53] Chernukhin, O. and Zingg, D. W., "Multimodality and Global Optimization in Aerodynamic Design," *AIAA Journal*, Vol. 51, No. 6, jun 2013, pp. 1342–1354.

[54] Poole, D. J., Allen, C. B., and Rendall, T. C. S., "A generic framework for handling constraints with agent-based optimization algorithms and application to aerodynamic design," *Optimization and Engineering*, 2016.

[55] Dugast, F., Favennec, Y., Josset, C., Fan, Y., and Luo, L., "Topology optimization of thermal fluid flows with an adjoint Lattice Boltzmann Method," *Journal of Computational Physics*, Vol. 365, 2018, pp. 376–404.

[56] Payot, A. D., Rendall, T., and Allen, C. B., "Restricted Snakes: a Flexible Topology Parameterisation Method for Aerodynamic Optimisation," *55th AIAA Aerospace Sciences Meeting, AIAA SciTech Forum, (AIAA 2017-1410)*, American Institute of Aeronautics and Astronautics, Reston, Virginia, jan 2017.

[57] Allen, C. B. and Rendall, T. C. S., "CFD-based optimization of hovering rotors using radial basis functions for shape parameterization and mesh deformation," *Optimization and Engineering*, Vol. 14, No. 1, Mar 2013, pp. 97–118.

[58] Gagnon, H. and Zingg, D., "Two-Level Free-Form Deformation for High-Fidelity Aerodynamic Shape Optimization," *14th AIAA/ISSMO Multidisciplinary Analysis and Optimization Conference*, 2012.

[59] Martins, J. R., Alonso, J. J., and Reuther, J. J., "A Coupled-Adjoint Sensitivity Analysis Method for High-Fidelity Aero-Structural Design," *Optimization and Engineering*, Vol. 6, No. 1, Mar 2005, pp. 33–62.

[60] van den Kieboom, K. T. H. and Elham, A., "Concurrent wing and high-lift system aerostructural optimization," *Structural and Multidisciplinary Optimization*, Vol. 57, No. 3, Mar 2018, pp. 947–963.

[61] Martins, J. and B. Lambe, A., "Multidisciplinary Design Optimization: A Survey of Architectures," *AIAA Journal*, Vol. 51, 09 2013, pp. 2049–2075.

[62] Kobbelt, L. P. and Bischoff, S., "Parameterization-free active contour models with topology control," *The Visual Computer*, Vol. 20, No. 4, jun 2004, pp. 217–228.

[63] Payot, A. D. J., Rendall, T. C. S., and Allen, C. B., "Restricted Snakes: a Flexible Topology Parameterisation Method for Aerodynamic Optimisation," *55th AIAA Aerospace Sciences Meeting*, 2017.

[64] Polak, E. and Ribiere, G., "Note sur la convergence de méthodes de directions conjuguées," *ESAIM: Mathematical Modelling and Numerical Analysis*, Vol. 3, No. 16, 1969, pp. 35–43.

[65] Storn, R. and Price, K., "Differential Evolution A Simple and Efficient Heuristic for Global Optimization over Continuous Spaces," *Journal of Global Optimization*, Vol. 11, No. 4, 1997, pp. 341–359.

[66] Mezura-Montes, E. and Coello Coello, C. a., "Constraint-handling in nature-inspired numerical optimization: Past, present and future," *Swarm and Evolutionary Computation*, Vol. 1, No. 4, dec 2011, pp. 173–194.

[67] Hecht, F., Pironneau, O., Le Hyaric, A., and Ohtsuka, K., "Freefem++ Manual," *J. Numer. Math.*, Vol. 20, 01 2012.

[68] Allaire, G. and Pantz, O., "Structural Optimization with FreeFem++," *Structural and Multidisciplinary Optimization*, Vol. 32, 09 2006.

[69] Zhu, B., Zhang, X., and Fatikow, S., "Structural topology and shape optimization using a level set method with distance-suppression scheme," *Computer Methods in Applied Mechanics and Engineering*, Vol. 283, 2015, pp. 1214 – 1239.

[70] Xia, Q., Wang, M. Y., and Shi, T., "A level set method for shape and topology optimization of both structure and support of continuum structures," *Computer Methods in Applied Mechanics and Engineering*, Vol. 272, 2014, pp. 340 – 353.

[71] Zhu, B., Zhang, X., and Fatikow, S., "Structural topology and shape optimization using a level set method with distance-suppression scheme," *Computer Methods in Applied Mechanics and Engineering*, Vol. 283, 2015, pp. 1214–1239.

[72] Wallin, M. and Ristinmaa, M., "Boundary effects in a phase-field approach to topology optimization," *Computer Methods in Applied Mechanics and Engineering*, Vol. 278, 2014, pp. 145 – 159.

[73] Carrasco, M., Ivorra, B., and Ramos, A. M., "Stochastic topology design optimization for continuous elastic materials," *Computer Methods in Applied Mechanics and Engineering*, Vol. 289, 2015, pp. 131 – 154.

[74] Valdez, S. I., Botello, S., Ochoa, M. A., Marroquín, J. L., and Cardoso, V., "Topology Optimization Benchmarks in 2D: Results for Minimum Compliance and Minimum Volume in Planar Stress Problems," *Archives of Computational Methods in Engineering*, Vol. 24, No. 4, Nov 2017, pp. 803–839.

[75] Steen Kristensen, E. and Flemming Madsen, N., "On the Optimum Shape of Fillets in Plates Subjected to Multiple In-Plane Loading Cases," *International Journal for Numerical Methods in Engineering*, Vol. 10, 01 1976, pp. 1007–1019.

[76] McKay, M. D., Beckman, R. J., and Conover, W. J., "A Comparison of Three Methods for Selecting Values of Input Variables in the Analysis of Output from a Computer Code," *Technometrics*, Vol. 21, No. 2, 1979, pp. 239–245.

[77] Makrizi, A., Radi, B., and ELHami, A., "Solution of the Topology Optimization Problem Based Subdomains Method," *Applied Mathematical Sciences*, Vol. 2, 01 2008, pp. 2029–2045.

[78] Strmberg, N., "Topology optimization of structures with manufacturing and unilateral contact constraints by minimizing an adjustable compliancevolume product," *Structural and Multidisciplinary Optimization*, Vol. 42, 09 2010, pp. 341–350.

[79] Payot, A. D., Rendall, T., and Allen, C. B., "Mixing and Refinement of Design Variables for Geometry and Topology Optimization in Aerodynamics," *35th AIAA Applied Aerodynamics Conference, AIAA AVIATION Forum, (AIAA 2017-3577)*, No. June, American Institute of Aeronautics and Astronautics, Reston, Virginia, jun 2017, pp. 1–24.